

Robust Survival Analysis with Adversarial Regularization

Michael Potter, *Student Member, IEEE*, Stefano Maxenti, *Student Member, IEEE*, Michael Everett, *Member, IEEE*

Abstract—Survival Analysis (SA) is about modeling the time for an event of interest to occur, which has important applications in many fields, including medicine, defense, finance, and aerospace. Recent work has demonstrated the benefits of using Neural Networks (NNs) to capture complicated relationships in SA. However, the datasets used to train these models are often subject to uncertainty (e.g., noisy measurements, human error), which we show can substantially degrade the performance of existing techniques. To address this issue, this work leverages recent advances in NN verification to provide new algorithms for generating fully-parametric survival models that are robust to such uncertainties. In particular, we introduce a robust loss function for training the models and use CROWN-IBP regularization to address the computational challenges with solving the resulting Min-Max problem. To evaluate the proposed approach, we apply relevant perturbations to publicly available datasets in the SurvSet repository and compare survival models against several baselines. We empirically show that Survival Analysis with Adversarial Regularization (SAWAR) method on average ranks best for dataset perturbations of varying magnitudes on metrics such as Negative Log Likelihood (NegLL), Integrated Brier Score (IBS), and Concordance Index (CI), concluding that adversarial regularization enhances performance in SA. Code: <https://github.com/mlpotter/SAWAR>

Index Terms—Survival Analysis, Adversarial Robustness, Neural Networks, Calibration, CROWN-IBP

I. INTRODUCTION

Survival Analysis (SA) is a highly active research field [1], [2] used to model the time before an event happens. For example, SA has been used extensively in medicine to quantify the effectiveness of various treatments as part of studies for cancer patients and drug trials [3]–[5]. While early approaches (dating back to the 1950s) predominantly used linear parametric models [6], [7], recent methods often leverage Neural Networks (NNs) to model complicated time-to-event data [8].

A key open challenge in this field is in developing models that are robust to uncertainty and variability in the datasets.

Michael Potter is a Ph.D. student at the Cognitive Systems Lab (CSL) inside the Centre for Spiral under the supervision of Prof. Deniz Erdogmus at Northeastern University, Boston. Email: potter.mi@northeastern.edu

Stefano Maxenti is a Ph.D. student at the Wireless Networks and Embedded Systems Lab (WiNES Lab) inside the Institute for the Wireless Internet of Things under the supervision of Prof. Tommaso Melodia at Northeastern University, Boston. Email: maxenti.s@northeastern.edu

Michael Everett is an Assistant Professor in Electrical and Computer Engineering at Northeastern University, Boston. Email: m.everett@northeastern.edu

©2024 IEEE. Personal use of this material is permitted. Permission from IEEE must be obtained for all other uses, in any current or future media, including reprinting/republishing this material for advertising or promotional purposes, creating new collective works, for resale or redistribution to servers or lists, or reuse of any copyrighted component of this work in other works. Submitted for review to: IEEE Journal - Transactions on Neural Networks and Learning Systems - 2024

Successful generalization of machine learning models over unseen datasets is crucial for clinical applications, as efficacy of developed drugs or treatments should be demonstrated over diverse patient demographics, institutions, and data acquisition settings [9]–[11]. Data uncertainty could be caused by human errors (e.g., notoriously poor handwriting of physicians [12], ineffective medical record keeping [13]), or inherent noise during transmissions or data collection [14]. However, many approaches assume perfect measurement of the covariates, ignoring aleatoric uncertainty [15]. In SA, the aleatoric uncertainty is only associated with the noise of the log of the measured time-to-event [6], [16]. Moreover, several studies have shown that adversaries can influence the final model to be over-/under-confident by purposefully poisoning studies or otherwise disrupting the data collection activities [17], [18]. Despite these known failure modes, and coupled with the sensitivity of NNs to input uncertainties, addressing the robustness of NNs against ϵ -perturbations trained specifically for fully-parametric SA remains unexplored.

To address these issues, this paper’s contributions include:

- identification of the sensitivity of existing SA methods, such as Deep Regularized Accelerated Failure Time (DRAFT) [19], to covariate perturbations via evaluating open-source datasets with a wide range of metrics related to predictive accuracy, calibration, and population curve estimation.
- our approach, Survival Analysis with Adversarial Regularization (SAWAR), which is the first method for enabling adversarial robustness to covariate perturbations within a bounded uncertainty set for fully-parametric NN-based SA. We improve calibration and stability on unexpected or noisy data by introducing a loss function based on a Min-Max formulation and Convex Relaxation Based Backward Bounding Pass with Interval Bound Propagation (CROWN-IBP) [20], [21].

The paper is structured as follows: Section II describes the State of the Art; Section III provides background to SA terminology and dataset structure; Section IV provides background on the adversarial and perturbation attacks used; Section V discusses the custom loss employed to deal with those attacks; Section VI provides the results of the experimental activity; finally, Section VII derives conclusions on our findings.

II. RELATED WORK

This section focuses on the literature about NNs for SA, with further detail about NN implementations available in a recent survey paper [22]. The first use of NNs in this field was a Feedforward Neural Network (FFNN) to approximate the

survival function [23], defined as the probability that no event occurs up to a specific time t . More recently, [24] proposed Cox-nnet, a NN that outputs a proportional-hazard [6], [25], which is the assumption that the difference in effect between different instances is constant as a function of time. Building on this idea, [26] developed DeepSurv, a Cox proportional-hazard NN for personalized treatment, which uses dropout layers to improve regularization and reduce overfitting. Instead of proportional hazard estimation, DeepWeiSurv [27] regresses the parameters of a Weibull mixture distribution with NNs.

Several recent works in SA aim to improve model calibration (e.g., by using new terms in the objective function [28]–[30]). A *calibrated* model provides a predicted confidence that is indicative of the true likelihood that the model is correct [31]. Meanwhile, few works have addressed adversarial robustness in SA. In general, a model is *adversarially robust* if small perturbations to the input do not cause the model to make incorrect predictions [32]. Adversarial robustness and model calibration are loosely coupled: while [33] showed that better calibration does not necessarily improve generalization, [34] showed that incorporating adversarial robustness during training improves trustworthiness in calibration and stability on unexpected data.

Existing adversarial training methods for SA face important tradeoffs between model complexity, performance, and ease of embedding of physical assumptions. Most of these techniques use Conditional Generative Adversarial Networks (CGANs) to generate samples of the time-to-event from a survival distribution in a non-parametric manner [19], [35], [36]. These models (e.g., CGANs) do not assume a functional form and define the survival distribution implicitly [37]–[39]. Therefore, there is no mathematical expression that describes the time-to-event Probability Density Function (PDF) value given covariates. One benefit of implicit models is that increased model complexity leads to increased flexibility, which is the ability to fit many other potential data realizations [40]. However, the higher model complexity generally violates the Bayesian Occam’s Razor, which penalizes models for having too much flexibility [40]. To satisfy the Bayesian Occam’s Razor’s “just right” model complexity, modeling assumptions known as *inductive biases* are employed in the form of an explicit *parametric* model [37], [39]. For example, a common inductive bias for SA models is the memoryless property [38], which the exponential distribution satisfies. For this reason, this paper uses the exponential distribution, which is commonly used in SA [41]–[43] (and more generally in queuing theory [44], [45], reliability analysis [8], [46], and telecommunications [45]).

III. PRELIMINARIES ON SURVIVAL ANALYSIS

SA [6], [25] is a statistical approach used to analyze and model the time $t \in \mathcal{R}_{++}$ until an event $e \in \{0, 1\}$ happens (e.g., a disease occurs, a device breaks). Typically, the study happens over a finite time period and instances/individuals may leave the study early before an event is recorded, with no follow up. In those cases, the dataset records that no event occurred up until the exit time of the study, which is

called *right censoring* [47]. Such an SA dataset consists of N independent instances/individuals, each denoted by index i , for which time between entry to a study and the subsequent event is recorded. Upon entry time to a study, the instance’s *covariates* $\mathbf{x}_i \in \mathcal{R}^d$ (i.e., variables that may affect the event of interest for the study) are measured. In summary, the dataset \mathcal{D} has the following structure:

$$\mathcal{D} = \{(\mathbf{x}_i, t_i, e_i)\}_{i=1}^N.$$

Being a statistical approach, we define the required probabilistic functions to model time-to-event data next.

A. Proportional Hazard Model

Let us denote T as a continuous, non-negative, random variable that represents the time-to-event, with PDF $f(t)$ and Cumulative Distribution Function (CDF) $F(t) = P[T \leq t]$. The survival function $S(t) := 1 - F(t)$ is the complement of this CDF [6], [48].

An exponential parametric survival model is expressed as

$$S(t) = e^{-\Lambda(t)}, \quad (1)$$

where $\Lambda(t) = \int_0^t \lambda(u)du$ is the cumulative hazard and

$$\lambda(t) = \frac{f(t)}{S(t)} = \lim_{\Delta \rightarrow 0} \frac{P[t < T < t + \Delta]}{\Delta} \quad (2)$$

is the instantaneous failure rate at time t .

To incorporate the instance’s covariates, we use the proportional hazard model [7], [49]. This model assumes that the covariates increase or decrease the hazard by a proportional amount at all times [6], [48],

$$\lambda_{\theta}(t, \mathbf{x}) = \lambda_0(t)e^{G_{\theta}(\mathbf{x})}, \quad (3)$$

where $\lambda_0(t)$ is a baseline hazard, $e^{G_{\theta}(\mathbf{x})}$ is the relative risk associated with covariates \mathbf{x} , and $G_{\theta}(\mathbf{x})$ is an NN with parameters θ in our setting.

The exponential proportional hazard model characterizes the baseline hazard rate as a constant function of time, and therefore $\lambda_0(t) = \lambda_0$. For simplicity, we assume an exponential baseline hazard, and we may “absorb” the λ term into the bias of the NN:

$$\lambda_0 e^{G_{\theta}(\mathbf{x})} = e^{\log \lambda_0 + G_{\theta}(\mathbf{x})} = e^{G_{\theta}(\mathbf{x})}. \quad (4)$$

The proportional hazard model PDF, CDF, and complement CDF for an exponential proportional hazard model are then given by:

$$\begin{aligned} f_{\theta}(t|\mathbf{x}) &= e^{G_{\theta}(\mathbf{x})} e^{-e^{G_{\theta}(\mathbf{x})}t} \\ F_{\theta}(t|\mathbf{x}) &= 1.0 - e^{-e^{G_{\theta}(\mathbf{x})}t} \\ S_{\theta}(t|\mathbf{x}) &= e^{-e^{G_{\theta}(\mathbf{x})}t}. \end{aligned}$$

$S_{\theta}(t|\mathbf{x})$ is also known as the instance survival function.

The population survival curve is the marginalization of the instance survival function over the covariates,

$$S(t) = \int S_{\theta}(t|\mathbf{x})p(\mathbf{x})d\mathbf{x}. \quad (5)$$

Since the distribution of the covariates $p(\mathbf{x})$ is typically unknown [50], the integral in Eq. (5) is often replaced with a Monte Carlo estimate [28]:

$$S(t) \approx \frac{1}{N} \sum_{i=1}^N S_{\theta}(t|\mathbf{x}_i). \quad (6)$$

B. Baseline Objective Functions

Given those definitions, the following loss functions enable finding model parameters θ from dataset \mathcal{D} . In particular, we follow [19], [51], [52] to define two objective functions based on negative log likelihood (Section III-B1) and the rank correlation (Section III-B2).

1) *Right Censored Log Likelihood Objective*: The \mathcal{L}_{LL} objective is the log of the time-to-event likelihood over \mathcal{D} specified by the proportional hazard model [6]:

$$\mathcal{L}_{LL}(\theta; \mathbf{X}, \mathbf{t}, \mathbf{e}) = \sum_{i=1}^N e_i \cdot \log f_{\theta}(t_i|\mathbf{x}_i) + \sum_{i=1}^N (1 - e_i) \cdot \log S_{\theta}(t_i|\mathbf{x}_i). \quad (7)$$

The first summation in Eq. (7) is the log likelihood of the datapoints corresponding to when the event occurs and the exact time of occurrence is observed. The second summation in Eq. (7) is the log likelihood when right censoring occurs.

2) *Ranking Objective*: The \mathcal{L}_{rank} objective is a ranking loss that penalizes an incorrect ordering of pairs $\{F_{\theta}(t_i|\mathbf{x}_i), F_{\theta}(t_j|\mathbf{x}_j)\}$, where instance i with event time $t_i < t_j$ should have a higher probability of failure than instance j at time t_i :

$$\mathcal{L}_{rank}(\theta; \mathbf{X}, \mathbf{t}, \mathbf{e}) = \sum_{i \neq j} A_{i,j} \eta \left(F_{\theta}(t_i|\mathbf{x}_i), F_{\theta}(t_j|\mathbf{x}_j) \right), \quad (8)$$

where $\eta(\mathbf{x}, \mathbf{y}) = \exp(-\frac{(\mathbf{x}-\mathbf{y})}{\sigma})$ and $A_{i,j}$ indicates an ‘‘acceptable’’ comparison pair [51]–[53]. We set $\sigma = 1$ for all experiments.

3) *Combined Objective*: The combined right censored negative log likelihood objective and the risk ranking objective, with risk ranking objective weight trade-off $w = \frac{1}{\text{batch_size}}$ is

$$\mathcal{L}(\theta; \mathbf{X}, \mathbf{t}, \mathbf{e}) = -\mathcal{L}_{LL}(\theta; \mathbf{X}, \mathbf{t}, \mathbf{e}) + w \cdot \mathcal{L}_{rank}(\theta; \mathbf{X}, \mathbf{t}, \mathbf{e}). \quad (9)$$

This combined objective provides a trade-off between finding the NN parameters θ that maximize the likelihood of observing \mathcal{D} and maximize a rank correlation between the instance risk scores and the observed failure times. We will denote the combined loss as the *baseline* objective. Our baseline model’s objective is similar to DRAFT [54] but with a different ranking objective function.

Thus far, we have described an objective function that improves predictive performance:

$$\theta^* = \arg \min_{\theta} \mathcal{L}(\theta; \mathbf{X}, \mathbf{t}, \mathbf{e}) \quad (10)$$

In the next section, we address how to develop NN models that are robust against adversarial attacks.

IV. PRELIMINARIES ON ADVERSARIAL TRAINING

Adversarial training [21], [32], [55], [56] is a technique to improve robustness and generalization of NNs to uncertain data. Rather than training on pristine data, adversarial training perturbs the data throughout the training process to encourage the model to optimize for parameters that are resilient against such perturbations. For example, [56] formulated adversarial training as solving a Min-Max robust optimization problem:

$$\min_{\theta} \max_{\tilde{\mathbf{X}}} \mathcal{L}(\theta; \tilde{\mathbf{X}}), \quad (11)$$

where $\tilde{\mathbf{X}} = \{\tilde{\mathbf{x}}_i \in \mathcal{B}(\mathbf{x}_i, \epsilon)\}_{i=1}^N$, and $\mathcal{B}(\mathbf{x}_i, \epsilon)$ is the ℓ_{∞} -ball of radius ϵ around \mathbf{x}_i .

In practice, the Min-Max problem posed in [56] is intractable to compute exactly. In particular, the inner maximization requires finding a global optimum over a high dimensional and non-convex loss function over NN parameters. Therefore, many recent adversarial training methods propose approximations to Eq. (11), leading to models with varying degrees of robustness to different data uncertainties. To understand the robustness properties of SA models to a variety of data uncertainties present in real applications, this paper investigates several perturbation methods, described next.

A. Certifiable Robustness

One such approximation is to use techniques from NN verification during training. For example, CROWN-IBP combines Convex Relaxation Based Backward Bounding Pass (CROWN) and Interval Bound Propagation (IBP) methods to obtain a convex relaxation for the lower bound and upper bound of each layer in the NN with respect to input data [55], [57]. CROWN-IBP is commonly used for verifying NN properties over a range of possible inputs. [55], [58] showed the linear relaxation may be extended to the entire objective function:

$$\max_{\tilde{\mathbf{X}}} \mathcal{L}(\tilde{\mathbf{X}}) \leq \bar{\mathcal{L}}(\tilde{\mathbf{X}}). \quad (12)$$

This relaxation has several benefits: it is convex with respect to the NN weights, which enables efficient optimization, and by optimizing over an upper bound on the inner maximization, this relaxation represents accounting for a strong adversary during training.

B. Adversarial Attacks

Another way to approximate Eq. (19) is to use adversarial attacks. Whereas CROWN-IBP provides an upper bound on the inner maximization (i.e., $\max_{\tilde{\mathbf{X}}} \mathcal{L}(\theta; \tilde{\mathbf{X}})$), adversarial attack algorithms typically provide a lower bound:

$$\max_{\tilde{\mathbf{X}}} \mathcal{L}(\theta; \tilde{\mathbf{X}}) \approx \mathcal{L}(\theta; \tilde{\mathbf{X}}_{FGSM}) \quad (13)$$

Fast Gradient Sign Method (FGSM) [59] uses the gradient of the objective function with respect to the input \mathbf{x} to perturb \mathbf{x} in the direction that maximizes the objective \mathcal{L} . Projected Gradient Descent (PGD) [56] iteratively applies that same type of first-order perturbation K times (or until convergence is reached), but constrains the perturbation to \mathbf{x} within a specified

set (e.g., ℓ_p -ball). FGSM is a special case of PGD, with $K = 1$ and the ℓ_∞ -ball.

Considering the structure of the datasets as described in Section III, we perturb only the covariates \mathbf{x} and not the time-to-event t . The perturbed covariates are calculated as:

$$\mathbf{x}^{(0)} = \mathbf{x} \quad (14)$$

$$\mathbf{x}^{(k+1)} = \Pi_{\mathcal{B}(\mathbf{x}, \epsilon)} \left(\mathbf{x}^{(k)} + \alpha (\nabla_{\mathbf{x}} \mathcal{L}(\boldsymbol{\theta}; \mathbf{x}^{(k)}, t, e)) \right), \quad (15)$$

$$\tilde{\mathbf{x}} = \mathbf{x}^{(K)}, \quad (16)$$

where k is the iteration step and α is a step size parameter.

C. Random Noise

While robustness to a worst-case perturbation is important for many applications, adding random noise to training data has also been shown to improve generalization performance [60]. Therefore, this paper also considers Gaussian Noise perturbations with variance ϵ bounded within an ℓ_∞ ball:

$$\mathbf{z} \sim \mathcal{N}(0, \mathbf{I}), \quad (17)$$

$$\tilde{\mathbf{x}} = \mathbf{x} + \Pi_{\mathcal{B}(0, \epsilon)}(\sqrt{\epsilon} \mathbf{I} \mathbf{z}). \quad (18)$$

We next introduce our approach, SAWAR, to incorporate adversarial regularization with SA models for improved calibration, predictive generalization, and adversarial robustness.

V. SURVIVAL ANALYSIS WITH ADVERSARIAL REGULARIZATION

As discussed in Section I, a key open challenge in SA is in developing models that are robust to uncertainty and variability in the datasets. This paper aims to improve the adversarial robustness of an NN against covariate perturbations within the SA framework. In doing so, this paper proposes the first method for enabling adversarial robustness for fully-parametric NN-based SA, which improves calibration and stability on unexpected or noisy data.

The following sections detail our approach, which extends the baseline objective function in Section III-B3 to include adversarial regularization posed as a Min-Max optimization problem in Section Section IV [21], [55].

A. Min-Max Formulation

When solving for $\boldsymbol{\theta}$ in SA, many approaches treat each measurement in dataset \mathcal{D} as ground-truth, ignoring aleatoric uncertainty [15]. Typically in SA, the aleatoric uncertainty is only associated with the noise of the log of the measured time-to-event (e.g. the Gumbel distribution or Log Normal distribution) [6], [16]. Instead, SAWAR approach assumes that each covariate is subject to a perturbation within a bounded uncertainty set, which leads to a robust optimization formulation as in Section IV. Thus, we optimize the NN parameters for the worst-case realizations of the baseline objective in Section III-B3:

$$\min_{\boldsymbol{\theta}} \max_{\tilde{\mathbf{X}}} \mathcal{L}(\boldsymbol{\theta}; \tilde{\mathbf{X}}, t, e). \quad (19)$$

As NNs are highly non-convex, solving this optimization problem is difficult [61]. Therefore, we use the adversarial training methods discussed in Section IV to approximate/relax the inner maximization term of the Min-Max formulation.

B. Adversarial Robustness Regularization

[21] shows that tight relaxations to the inner maximization of a Min-Max problem may over-regularize the NN, leading to poor predictive performance. Therefore, we extend the baseline objective in Eq. (9) with the adversarial robustness objective in Eq. (19) [55], [57] to balance predictive performance and adversarial robustness as:

$$\min_{\boldsymbol{\theta}} \left[\kappa \cdot \mathcal{L} + (1 - \kappa) \cdot \max_{\tilde{\mathbf{X}}} \mathcal{L} \right], \quad (20)$$

where $\kappa \in (0, 1)$.

We propose to use the open-source library *auto_LiRPA* [58] to relax the inner maximization term of the adversarial regularization with CROWN-IBP. *auto_LiRPA* seamlessly integrates with PyTorch for automatic backpropagation, computing a fully differentiable upper bound on the inner maximization term of Eq. (20) in a computationally feasible manner.

C. SAWAR Training

We show the pseudo-code in Algorithm 1. The NN parameters are updated using stochastic gradient descent with the ADAM optimizer [62] (Line 12), where we use early stopping [63] with respect to the validation set to prevent overfitting (Lines 24 to 26). We introduce the covariate perturbation attacks after 100 epochs (Lines 4 to 7). A smooth ϵ -scheduler linearly increases the ϵ -perturbation magnitude from 0.0 to 0.5 within a 30 epoch window (Line 27) after 100 epochs. We do not allow early stopping until after the maximum ϵ -perturbation magnitude is achieved.

Algorithm 1 Robust Training with CROWN-IBP

```

1: procedure TRAIN_STEP(ModelLoss, Data,  $\epsilon$ ,  $\kappa$ , Train)
2:    $loss_{epoch} \leftarrow 0$ 
3:   for  $x_B, t_B, y_B$  in Data do
4:     if  $\epsilon > 1e^{-20}$  then
5:        $loss_{natural} \leftarrow \text{ModelLoss}(x_B, t_B, e_B)$ 
6:        $\tilde{x}_B \leftarrow \text{PerturbationLpNorm}(x_B, \epsilon)$ 
7:        $loss_{robust} \leftarrow \text{CROWN-IBP}(\text{ModelLoss})(\tilde{x}_B, t_B, e_B)$ 
8:        $loss \leftarrow \kappa \times loss_{natural} + (1 - \kappa) \times loss_{robust}$ 
9:     else
10:       $loss \leftarrow \text{ModelLoss}(x_B, t_B, e_B)$ 
11:   if Train then
12:     ADAM Optimizer Step with  $loss.backward()$ 
13:    $loss_{epoch} \leftarrow loss_{epoch} + loss$ 
14:   return  $loss_{epoch}$ 

15: procedure TRAIN_ROBUST(Model, Datatr, Dataval,  $\kappa$ )
16:   Init random seeds, ADAM optimizer, lr-scheduler,  $\epsilon$ -scheduler
17:   ModelLoss = LossWrapper(Model)
18:    $loss_{best} \leftarrow \infty$ 
19:   for  $t$  in Epochs do
20:     if  $\epsilon$ -scheduler reached  $\epsilon_{max}$  then
21:       lr-scheduler Step
22:      $loss_{tr} \leftarrow \text{TRAIN\_STEP}(\text{ModelLoss}, \text{Data}_{tr}, \epsilon, \kappa, \text{True})$ 
23:      $loss_{val} \leftarrow \text{TRAIN\_STEP}(\text{ModelLoss}, \text{Data}_{val}, \epsilon, \kappa, \text{False})$ 
24:     if  $loss_{val} \leq loss_{best}$  then
25:       Save Best Model
26:        $loss_{best} \leftarrow loss_{val}$ 
27:      $\epsilon$ -scheduler Step
28:   return Model

```

We expect that the model’s adversarial robustness and predictive calibration should increase when incorporating data uncertainty in SAWAR objective [34] via the adversarial regularization term in Eq. (20) and illustrate SAWAR hypothesis via extensive experiments in the next section.

VI. EXPERIMENTS

We conduct experiments over 10 benchmark SA datasets (VI-B) to quantify the impact of perturbation after the robust training is complete. As evaluation metrics, we consider the Concordance Index (CI) [64], the Integrated Brier Score (IBS) [65] and the Negative Log Likelihood (NegLL) at varying ϵ -perturbation magnitudes from 0 to 1. We show that SAWAR improves predictive accuracy, calibration, and population curve estimation.

A. Configuration

The experiments are conducted on a 12th Gen Intel(R) Core (TM) 16 GB RAM i9-12900 processor running a Windows operating system. Each dataset undergoes stratified partitioning into train, validation, test sets with proportions 60%, 20%, 20% respectively. The NN G_θ has two hidden layers of 50 neurons each and *Leaky ReLU* activation functions. *lifelines* [66], and *sksurv* [53] software packages are employed to ensure standardization and reproducibility in computing the SA metrics.

B. Datasets

We use the open-source API *SurvSet* [67], to download the benchmark SA datasets shown in Table I.

Dataset	N	n_{fac}	n_{ohe}	n_{num}
TRACE	1878	4	4	2
stagec	146	4	15	3
flchain	7874	4	26	6
Aids2	2839	3	11	1
Framingham	4699	2	12	5
dataDIVAT1	5943	3	14	2
prostate	502	6	16	9
zinc	431	11	18	2
retinopathy	394	5	9	2
LeukSurv	1043	2	24	5

TABLE I: Studied datasets from *SurvSet*. n_{fac} is the number of categorical features, n_{ohe} is number of binary features (one-hot-encoded) and n_{num} is number of numerical features.

- 1) The **TRACE** [68] dataset is from a study on a subset of patients admitted after myocardial infarction to examine various risk factors.
- 2) The **stagec** [69] dataset is from a study exploring the prognostic value of flow cytometry for patients with stage C prostate cancer.
- 3) The **flchain** [70] dataset is from a study on the relationship between serum free light chain (FLC) and mortality of Olmsted Country residents aged 50 years or more.
- 4) The **Aids2** [71] dataset is from patients diagnosed with AIDS in Australia before 1 July 1991.
- 5) The **Framingham** [72] dataset is from the first prospective study of cardiovascular disease with identification of risk factors and joint effects.

- 6) The **dataDIVAT1** [73] dataset is from the first sample from the DIVAT Data Bank for French kidney transplant recipients from DIVAT cohort.
- 7) The **prostate** [74] dataset is from a randomised clinical trial comparing treatment for patients with stage 3 and stage 4 prostate cancer.
- 8) The **zinc** [75] is from the first study to examine association between tissue elemental zinc levels and the esophageal squamous cell carcinoma.
- 9) The **retinopathy** [76] is from the trial of laser coagulation as treatment to delay diabetic retinopathy.
- 10) The **LeukSurv** [77] is from the study on survival of acute myeloid leukemia and connection to spatial variation in survival.

We preprocess each dataset by one-hot encoding categorical covariates, followed by standard normalizing all covariates.

C. Adversary Setup

A detailed insight into the robust evaluation procedure is shown in Algorithm 2. We use two adversarial attack methods when benchmarking the robustness of the adversarial regularization method (Lines 13, 14 and 18): FGSM attack (Section IV-B) and a novel worst-case attack. We define the worst-case attack as the maximum failure rate with respect to the covariate uncertainty:

$$\tilde{\lambda}_\theta = \max_{\tilde{\mathbf{x}}_i \in \mathcal{B}(\mathbf{x}_i, \epsilon)} e^{G_\theta(\tilde{\mathbf{x}}_i)}, \quad (21)$$

and define the ϵ -worst-case survival curve as:

$$\tilde{S}(t|\mathbf{x}) = e^{-\tilde{\lambda}_\theta t}, \quad (22)$$

which is the lowest survival probability at a given time t with respect to the ϵ -perturbed input covariates. For the exponential distribution, as the failure rate increases with the ϵ -perturbation, the probability of survival decreases monotonically. We use CROWN-IBP for a tight approximation to the upper bound on the maximization term in equation Eq. (21). We evaluate the SA metrics for $\epsilon \in [0, 1]$ for the two attacks methods to study how sensitive each adversarial training method is to covariate perturbation (Line 1).

Note that when the activation functions are piecewise linear, an exact solution can also be obtained by solving a Mixed Integer Linear Program (MILP). However, solving the MILP is computationally prohibitive: even for $\epsilon = 0.1$ each MILP takes on average 9-10 seconds when tested on the Dialysis dataset, whereas CROWN-IBP takes milliseconds to calculate over all the data in the Dialysis dataset.

D. Results

Furthermore, we analyze how these adversarial attacks impact the characteristics of the population survival curves.

1) *Failure Rate Distribution*: Let us assume that the input covariates are random variables. Then the failure rate becomes a random variable that occurs from the stochasticity of the

ϵ	Concordance Index					Integrated Brier Score					Negative Log Likelihood				
	baseline	noise	fgsm	pgd	SAWAR	baseline	noise	fgsm	pgd	SAWAR	baseline	noise	fgsm	pgd	SAWAR
1.00	<u>2.9</u>	3.35	3.35	2.5	<u>2.9</u>	4.6	4.4	2.4	<u>1.9</u>	1.7	4.0	4.7	2.7	<u>2.1</u>	1.5
0.90	<u>3.1</u>	3.5	3.45	2.45	<u>2.5</u>	4.5	4.5	2.5	<u>1.8</u>	1.7	4.0	4.7	2.9	<u>1.9</u>	1.5
0.80	3.4	3.4	3.2	2.35	<u>2.65</u>	4.6	4.4	2.6	<u>1.8</u>	1.6	4.1	4.6	3.0	<u>1.9</u>	1.4
0.70	3.45	3.35	3.1	2.4	<u>2.7</u>	4.7	4.3	2.6	<u>1.8</u>	1.6	4.2	4.5	3.0	<u>2.0</u>	1.3
0.60	3.45	3.45	3.0	2.5	<u>2.6</u>	4.7	4.3	2.7	<u>1.8</u>	1.5	4.2	4.5	3.1	<u>2.1</u>	1.1
0.50	3.85	3.65	3.1	2.1	<u>2.3</u>	4.4	4.6	2.9	<u>1.8</u>	1.3	4.1	4.5	3.2	<u>2.1</u>	1.1
0.40	3.9	3.8	3.05	2.1	<u>2.15</u>	4.4	4.6	3.0	<u>1.9</u>	1.1	4.0	4.6	3.2	<u>2.1</u>	1.1
0.30	4.4	4.2	3.0	<u>1.9</u>	1.5	4.4	4.6	3.0	<u>1.9</u>	1.1	4.0	4.6	3.2	<u>2.1</u>	1.1
0.20	4.35	4.0	3.3	<u>2.25</u>	1.1	4.2	4.6	3.2	<u>2.0</u>	1.0	3.9	4.7	3.2	<u>2.1</u>	1.1
0.10	4.25	4.0	3.3	<u>2.35</u>	1.1	4.0	4.6	3.2	<u>2.2</u>	1.0	3.8	4.8	3.1	<u>2.3</u>	1.0
0.05	3.85	4.0	3.45	<u>2.6</u>	1.1	3.8	4.7	2.9	<u>2.2</u>	1.4	3.9	4.7	3.1	<u>2.3</u>	1.0
0.00	<u>2.95</u>	3.95	3.35	3.35	1.4	3.0	3.9	3.3	<u>2.5</u>	2.3	<u>2.6</u>	4.1	3.5	2.8	2.0

TABLE II: FGSM average ranks for CI, IBS, and NegLL metrics across all datasets. Lower number is better.

ϵ	Concordance Index					Integrated Brier Score					Negative Log Likelihood				
	baseline	noise	fgsm	pgd	SAWAR	baseline	noise	fgsm	pgd	SAWAR	baseline	noise	fgsm	pgd	SAWAR
1.00	<u>2.8</u>	3.4	3.5	3.6	1.7	<u>2.6</u>	4.3	3.8	3.3	1.0	3.1	4.5	3.4	<u>3.0</u>	1.0
0.90	<u>3.1</u>	3.3	3.5	3.4	1.7	<u>3.0</u>	4.3	3.6	3.1	1.0	3.1	4.5	3.5	<u>2.9</u>	1.0
0.80	<u>3.0</u>	3.3	3.5	3.7	1.5	<u>3.0</u>	4.5	3.5	<u>3.0</u>	1.0	3.0	4.6	3.5	<u>2.9</u>	1.0
0.70	<u>3.05</u>	3.3	3.6	3.65	1.4	<u>3.0</u>	4.5	3.5	<u>3.0</u>	1.0	3.1	4.5	3.5	<u>2.9</u>	1.0
0.60	<u>2.85</u>	3.55	3.55	3.75	1.3	<u>3.0</u>	4.5	3.5	<u>3.0</u>	1.0	3.0	4.7	3.5	<u>2.8</u>	1.0
0.50	<u>3.2</u>	3.9	3.35	3.45	1.1	3.2	4.4	3.5	<u>2.9</u>	1.0	3.0	4.7	3.5	<u>2.8</u>	1.0
0.40	3.25	3.95	<u>3.2</u>	3.5	1.1	3.3	4.8	3.2	<u>2.7</u>	1.0	3.1	4.7	3.4	<u>2.8</u>	1.0
0.30	<u>3.0</u>	3.05	3.95	3.6	1.4	3.5	4.7	3.3	<u>2.5</u>	1.0	3.3	4.9	3.2	<u>2.6</u>	1.0
0.20	<u>2.05</u>	2.95	4.2	3.8	2.0	3.7	4.7	3.4	<u>2.2</u>	1.0	3.4	4.9	3.4	<u>2.3</u>	1.0
0.10	<u>2.85</u>	3.4	3.4	3.35	2.0	3.3	4.5	3.0	<u>2.3</u>	1.9	3.5	4.5	3.2	<u>2.2</u>	1.6
0.05	3.05	4.15	3.4	<u>2.9</u>	1.5	<u>2.6</u>	4.4	3.0	<u>2.6</u>	2.4	3.3	4.4	3.0	<u>2.4</u>	1.9
0.00	<u>2.95</u>	3.95	3.35	3.35	1.4	3.0	3.9	3.3	<u>2.5</u>	2.3	<u>2.6</u>	4.1	3.5	2.8	2.0

TABLE III: Worst-Case average ranks for CI, IBS, and NegLL metrics across all datasets. Lower number is better.

Algorithm 2 Adversarial Robustness Evaluation

```

1: procedure EVAL_ROBUST(Model, Data, Metric, Method,  $\epsilon$ )
2:    $X, t, e = \text{Data}$ 
3:   MetricValues=[]
4:   for  $\epsilon$  in 0 : 0.1 : 1 do
5:     if  $\epsilon = 0$  then
6:        $\lambda_\theta \leftarrow \text{Model}(X)$ 
7:       MetricValues = [MetricValues, Metric( $\lambda_\theta, t, e$ )]
8:     else
9:        $\tilde{\lambda}_\theta \leftarrow \text{ATTACK}(\text{Model}, \text{Data}, \text{Method}, \epsilon)$ 
10:      MetricValues = [MetricValues, Metric( $\tilde{\lambda}_\theta, t, e$ )]
11:   return MetricValues

12: procedure ATTACK(Model, Data, Method,  $\epsilon$ )
13:    $X, t, e = \text{Data}$ 
14:   if Method = FGSM then
15:     ModelLoss = LOSSwrapper(Model)
16:      $\tilde{X} \leftarrow \text{FGSM}(\text{ModelLoss}, X, t, e, \epsilon)$ 
17:      $\tilde{\lambda}_\theta \leftarrow \text{Model}(\tilde{X})$ 
18:   if Method = worst-case then
19:      $\tilde{X} \leftarrow \text{PerturbationLpNorm}(X, \epsilon)$ 
20:      $\tilde{\lambda}_\theta \leftarrow \text{CROWN-IBP}(\text{Model})(\tilde{X}, t, e)$ 
21:   return  $\tilde{\lambda}_\theta$ 

```

input covariates. Moreover, we may treat $S_\theta(t|\mathbf{x})$ as a stochastic process:

$$\mathbf{x} \sim p(\mathbf{x}); \lambda \sim \lambda_\theta(\mathbf{x}) \quad (23)$$

$$S_\theta(t) \sim e^{-\lambda t} \quad (24)$$

Furthermore, we compute statistical quantities such as expectation, lower 5th quantile, and upper 95th quantile:

$$LB = Q_{05}(\lambda_\theta(\mathbf{x})), \quad (25)$$

$$UB = Q_{95}(\lambda_\theta(\mathbf{x})). \quad (26)$$

Fig. 1 visualizes the credible interval and mean of the survival function stochastic process in Eq. (24). The 90% credible interval of the the stochastic process changes with respect to the strength of the adversarial regularization method (Fig. 1). We observe the trend that the credible interval slightly narrows down as the strength of the adversarial regularization method increases (Fig. 1). The variance of the failure rate decreasing leads to a more robust model against adversarial attacks. For example, when $\text{Var}(\lambda_\theta(\mathbf{x})) = 0$, then there is a mode collapse such that $\lambda(\mathbf{x}_i) = \lambda \forall i$. This is the case for point-estimates of the parameter λ derived via maximum likelihood estimation. A point-estimate results in a population curve, but no instance-level survival curves. Therefore, by utilizing a weighted objective in Eq. (20), we trade-off individualized survival curves with vulnerability to adversarial attacks and a population survival curve which is completely resilient to adversarial attacks.

However, despite exhibiting significantly higher adversarial robustness, the credible interval remains relatively unchanged compared to the baseline method.

2) *Population Survival Curve*: The ϵ -perturbation magnitude determines the severity of the worst-case survival curve. We observe the trend that the stronger the adversarial regularization method, the "closer" the ϵ -worst-case population curve becomes to the unperturbed population survival curve for a given $\epsilon \in [0, 1]$ (Fig. 2). Moreover, we use the Kaplan Meier Curve (KMC), a commonly used frequentist approach for non-parametrically estimating the population survival curve using samples $\{t_i, e_i\}_{i=1}^N$, to visually evaluate model calibration. The close alignment between the population survival curve and the KMC shown in Fig. 2 demonstrates the strong calibration of SAWAR model [29].

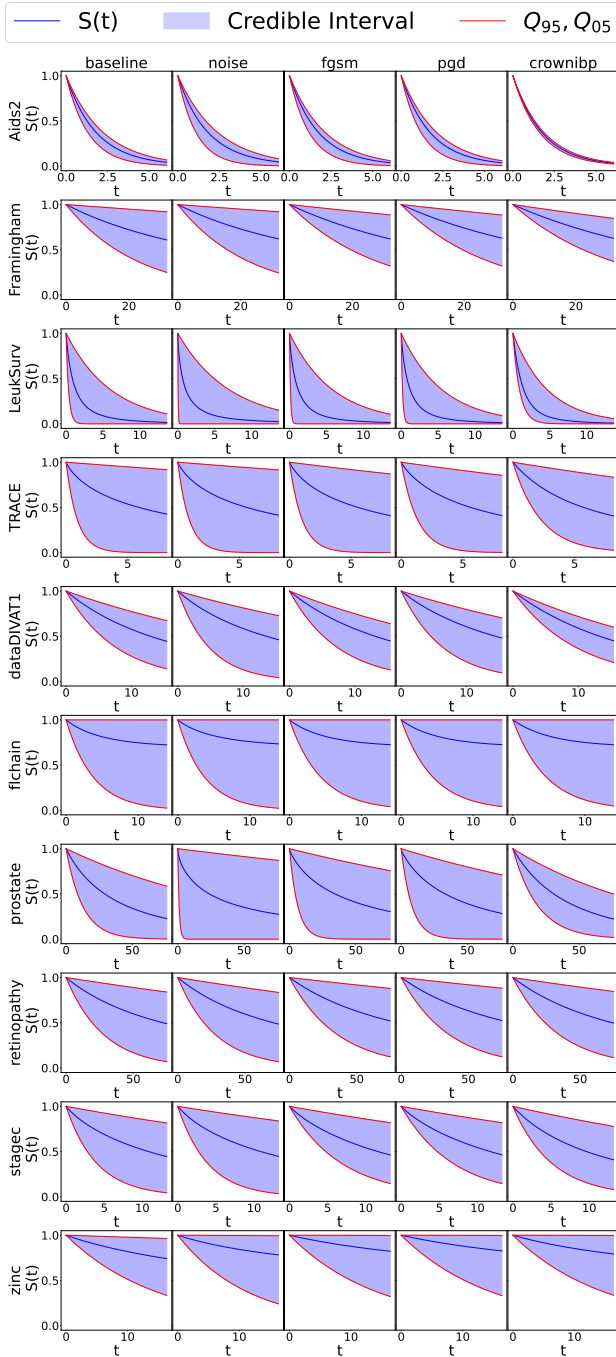


Fig. 1: Distribution of survival curves for baseline, noise, FGSM, PGD, and CROWN-IBP. As the strength of the adversarial training method increases, from left to right column, the 90% credible interval narrows. However, the credible interval of SAWAR does not drastically differ from the baseline.

We calculate the average ranking of each adversarial regularization method across all datasets with respect to CI, IBS, NegLL in response to the FGSM and ϵ -worst-case attacks (Tables II and III). We empirically showed that CROWN-IBP adversarial regularization leads to increased performance, consistently ranking the best across various ϵ -perturbation magnitudes.

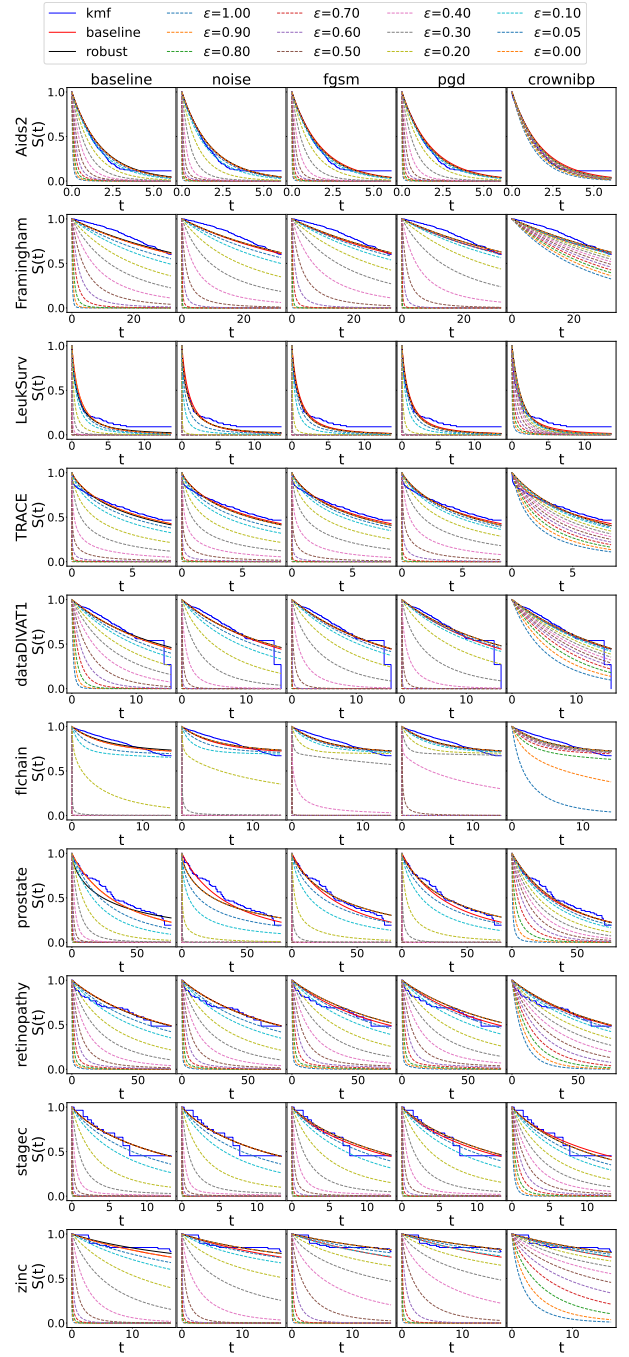


Fig. 2: Adversarial robustness of survival curves for baseline, noise, FGSM, PGD, and CROWN-IBP training against ϵ -worst-case attack. As the strength of the adversarial training method increases, from left to right column, the perturbed population survival curve for a given ϵ is closer to the KMC.

The exact corresponding metric values for each ϵ of the worst-case attack are provided in Appendix A.

VII. CONCLUSIONS

This paper is the first to introduce CROWN-IBP regularization for adversarial robustness training in SA with fully-parametric NN models. We benchmarked SAWAR method

on 10 time-to-event datasets with standard adversarial regularization methods such as Gaussian Noise, FGSM, and PGD against the FGSM and worst-case attack. SAWAR’s empirical results indicate that CROWN-IBP regularization consistently enhances performance in SA with respect to CI and IBS, and NegLL for all ϵ -perturbation magnitudes from 0 to 1. Moreover, compared to conventional adversarial regularization methods, SAWAR empirical evidence demonstrates that CROWN-IBP regularization is more resilient to input covariate perturbation attacks, where we see relative improvements to the baseline in CI and IBS of 1%-150% across all ϵ -perturbation magnitudes (Appendix A). Thus adversarial regularization improves predictive performance, adversarial robustness, and calibration.

Future work will include the use the Weibull Proportional Hazard model to enable time varying hazard rates. This will require extending auto_LiRPA to handle the power operator for operations such as t^k , where k is a learnable parameter.

REFERENCES

- [1] P. Wang, Y. Li, and C. K. Reddy, “Machine Learning for Survival Analysis: A Survey,” *ACM Comput. Surv.*, vol. 51, no. 6, feb 2019. [Online]. Available: <https://doi.org/10.1145/3214306>
- [2] S. Salerno and Y. Li, “High-dimensional survival analysis: Methods and applications,” *Annual review of statistics and its application*, vol. 10, pp. 25–49, 2023.
- [3] J. B. Greenhouse, D. Stangl, and J. Bromberg, “An introduction to survival analysis: statistical methods for analysis of clinical trial data.” *Journal of Consulting and Clinical Psychology*, vol. 57, no. 4, p. 536, 1989.
- [4] C. Brard, G. Le Teuff, M.-C. Le Deley, and L. V. Hampson, “Bayesian survival analysis in clinical trials: What methods are used in practice?” *Clinical Trials*, vol. 14, no. 1, pp. 78–87, 2017.
- [5] D. Altman, B. De Stavola, S. Love, and K. Stepniwska, “Review of survival analyses published in cancer journals,” *British journal of cancer*, vol. 72, no. 2, pp. 511–518, 1995.
- [6] D. G. Kleinbaum and M. Klein, *Survival analysis a self-learning text*. Springer, 1996.
- [7] D. R. Cox, “The regression analysis of binary sequences,” *Journal of the Royal Statistical Society Series B: Statistical Methodology*, vol. 20, no. 2, pp. 215–232, 1958.
- [8] B. Cheng and M. Potter, “Bayesian Weapon System Reliability Modeling with Cox-Weibull Neural Network,” in *2023 Annual Reliability and Maintainability Symposium (RAMS)*, 2023, pp. 1–6.
- [9] R. C. Deo, “Machine learning in medicine,” *Circulation*, vol. 132, no. 20, pp. 1920–1930, 2015.
- [10] G. Handelman, H. Kok, R. Chandra, A. Razavi, M. Lee, and H. Asadi, “ed octor: machine learning and the future of medicine,” *Journal of internal medicine*, vol. 284, no. 6, pp. 603–619, 2018.
- [11] A. Qayyum, J. Qadir, M. Bilal, and A. Al-Fuqaha, “Secure and robust machine learning for healthcare: A survey,” *IEEE Reviews in Biomedical Engineering*, vol. 14, pp. 156–180, 2020.
- [12] F. J. Rodríguez-Vera, Y. Marín, A. Sánchez, C. Borrachero, and E. Pujol, “Illegible handwriting in medical records,” *J R Soc Med*, vol. 95, no. 11, pp. 545–546, Nov 2002.
- [13] J. Li, Y. Mao, and J. Zhang, “Maintenance and quality control of medical equipment based on information fusion technology,” *Comput Intell Neurosci*, vol. 2022, p. 9333328, Oct 2022.
- [14] E. R. Lenz, *Measurement in nursing and health research*. Springer publishing company, 2010.
- [15] L. V. Utkin, V. S. Zaborovsky, M. S. Kovalev, A. V. Konstantinov, N. A. Politayeva, and A. A. Lukashin, “Uncertainty interpretation of the machine learning survival model predictions,” *IEEE Access*, vol. 9, pp. 120 158–120 175, 2021.
- [16] E. Liu and K. Lim, “Using the weibull accelerated failure time regression model to predict time to health events,” *bioRxiv*, 2018. [Online]. Available: <https://www.biorxiv.org/content/early/2018/08/27/362186>
- [17] G. Loukas, *Cyber-physical attacks: A growing invisible threat*. Butterworth-Heinemann, 2015.
- [18] A. Schwarzschild, M. Goldblum, A. Gupta, J. P. Dickerson, and T. Goldstein, “Just how toxic is data poisoning? a unified benchmark for backdoor and data poisoning attacks,” in *International Conference on Machine Learning*. PMLR, 2021, pp. 9389–9398.
- [19] P. Chapfuwa, C. Tao, C. Li, C. Page, B. Goldstein, L. C. Duke, and R. Henao, “Adversarial time-to-event modeling,” in *Proceedings of the 35th International Conference on Machine Learning*, ser. Proceedings of Machine Learning Research, J. Dy and A. Krause, Eds., vol. 80. PMLR, 10–15 Jul 2018, pp. 735–744. [Online]. Available: <https://proceedings.mlr.press/v80/chapfuwa18a.html>
- [20] S. Wang, H. Zhang, K. Xu, X. Lin, S. Jana, C.-J. Hsieh, and J. Z. Kolter, “Beta-crown: Efficient bound propagation with per-neuron split constraints for neural network robustness verification,” *Advances in Neural Information Processing Systems*, vol. 34, pp. 29 909–29 921, 2021.
- [21] H. Zhang, H. Chen, C. Xiao, S. Goyal, R. Stanforth, B. Li, D. Boning, and C.-J. Hsieh, “Towards stable and efficient training of verifiably robust neural networks,” 2019.
- [22] S. Wiegrefe, P. Kopper, R. Sonabend, B. Bischl, and A. Bender, “Deep Learning for Survival Analysis: A Review,” 2023.
- [23] D. Faraggi and R. Simon, “A neural network model for survival data,” *Statistics in Medicine*, vol. 14, no. 1, pp. 73–82, 1995. [Online]. Available: <https://onlinelibrary.wiley.com/doi/abs/10.1002/sim.4780140108>
- [24] T. Ching, X. Zhu, and L. X. Garmire, “Cox-nnet: An artificial neural network method for prognosis prediction of high-throughput omics data,” *PLOS Computational Biology*, vol. 14, no. 4, pp. 1–18, 04 2018. [Online]. Available: <https://doi.org/10.1371/journal.pcbi.1006076>
- [25] J. P. Klein and P. Goel, “Survival analysis: state of the art,” 1992.
- [26] J. L. Katzman, U. Shaham, A. Cloninger, J. Bates, T. Jiang, and Y. Kluger, “Deepsurv: personalized treatment recommender system using a cox proportional hazards deep neural network,” *BMC Medical Research Methodology*, vol. 18, no. 1, p. 24, Feb 26 2018. [Online]. Available: <https://doi.org/10.1186/s12874-018-0482-1>
- [27] A. Bennis, S. Mouysset, and M. Serrurier, “Estimation of conditional mixture weibull distribution with right censored data using neural network for time-to-event analysis,” in *Advances in Knowledge Discovery and Data Mining: 24th Pacific-Asia Conference, PAKDD 2020, Singapore, May 11–14, 2020, Proceedings, Part I 24*. Springer, 2020, pp. 687–698.
- [28] H. Haider, B. Hoehn, S. Davis, and R. Greiner, “Effective ways to build and evaluate individual survival distributions,” *The Journal of Machine Learning Research*, vol. 21, no. 1, pp. 3289–3351, 2020.
- [29] M. Goldstein, X. Han, A. Puli, A. Perotte, and R. Ranganath, “X-cal: Explicit calibration for survival analysis,” *Advances in neural information processing systems*, vol. 33, pp. 18 296–18 307, 2020.
- [30] F. Kamran and J. Wiens, “Estimating calibrated individualized survival curves with deep learning,” in *Proceedings of the AAAI Conference on Artificial Intelligence*, vol. 35, no. 1, 2021, pp. 240–248.
- [31] C. Guo, G. Pleiss, Y. Sun, and K. Q. Weinberger, “On calibration of modern neural networks,” in *International conference on machine learning*. PMLR, 2017, pp. 1321–1330.
- [32] I. J. Goodfellow, J. Shlens, and C. Szegedy, “Explaining and harnessing adversarial examples,” *arXiv preprint arXiv:1412.6572*, 2014.
- [33] R. Vasilev and A. D’yakonov, “Calibration of neural networks,” 2023.
- [34] Y. Qin, X. Wang, A. Beutel, and E. Chi, “Improving calibration through the relationship with adversarial robustness,” *Advances in Neural Information Processing Systems*, vol. 34, pp. 14 358–14 369, 2021.
- [35] T. Uemura, J. J. Näppi, C. Watari, T. Hironaka, T. Kamiya, and H. Yoshida, “Weakly unsupervised conditional generative adversarial network for image-based prognostic prediction for covid-19 patients based on chest ct,” *Medical Image Analysis*, vol. 73, p. 102159, 2021. [Online]. Available: <https://www.sciencedirect.com/science/article/pii/S136184152100205X>
- [36] P. Liu, L. Ji, F. Ye, and B. Fu, “Advml: Adversarial multiple instance learning for the survival analysis on whole-slide images,” *Medical Image Analysis*, vol. 91, p. 103020, 2024. [Online]. Available: <https://www.sciencedirect.com/science/article/pii/S1361841523002803>
- [37] A. Zellner, H. A. Keuzenkamp, and M. McAleer, *Simplicity, inference and modelling: Keeping it sophisticatedly simple*. Cambridge University Press, 2002.
- [38] C. M. Bishop and N. M. Nasrabadi, *Pattern recognition and machine learning*. Springer, 2006, vol. 4, no. 4.
- [39] I. Goodfellow, “Nips 2016 tutorial: Generative adversarial networks,” 2017.
- [40] K. P. Murphy, *Machine learning: a probabilistic perspective*. MIT press, 2012.

- [41] R. Bender, T. Augustin, and M. Blettner, "Generating survival times to simulate cox proportional hazards models," *Statistics in medicine*, vol. 24, no. 11, pp. 1713–1723, 2005.
- [42] C. Stanley, E. Molyneux, and M. Mukaka, "Comparison of performance of exponential, cox proportional hazards, weibull and frailty survival models for analysis of small sample size data," *Journal of Medical Statistics and Informatics*, vol. 4, no. 1, 2016.
- [43] P. Royston, "Flexible parametric alternatives to the cox model, and more," *The Stata Journal*, vol. 1, no. 1, pp. 1–28, 2001.
- [44] L. Kleinrock, *Theory, Volume 1, Queueing Systems*. USA: Wiley-Interscience, 1975.
- [45] R. B. Cooper, "Queueing theory," in *Proceedings of the ACM'81 conference*, 1981, pp. 119–122.
- [46] K. Das, "A comparative study of exponential distribution vs weibull distribution in machine reliability analysis in a cms design," *Computers & Industrial Engineering*, vol. 54, no. 1, pp. 12–33, 2008.
- [47] S. P. Jenkins, "Survival analysis," *Unpublished manuscript, Institute for Social and Economic Research, University of Essex, Colchester, UK*, vol. 42, pp. 54–56, 2005.
- [48] G. Rodriguez, "Parametric survival models," *Rapport technique, Princeton: Princeton University*, 2010.
- [49] D. R. Cox, "Regression Models and Life-Tables," *Journal of the Royal Statistical Society. Series B (Methodological)*, vol. 34, no. 2, pp. 187–220, 1972. [Online]. Available: <http://www.jstor.org/stable/2985181>
- [50] W. Lowe, "Rare events research," in *Encyclopedia of Social Measurement*, K. Kempf-Leonard, Ed. New York: Elsevier, 2005, pp. 293–297. [Online]. Available: <https://www.sciencedirect.com/science/article/pii/B0123693985005570>
- [51] C. Lee, J. Yoon, and M. Van Der Schaar, "Dynamic-deephit: A deep learning approach for dynamic survival analysis with competing risks based on longitudinal data," *IEEE Transactions on Biomedical Engineering*, vol. 67, no. 1, pp. 122–133, 2019.
- [52] C. Lee, W. Zame, J. Yoon, and M. Van Der Schaar, "Deephit: A deep learning approach to survival analysis with competing risks," in *Proceedings of the AAAI conference on artificial intelligence*, vol. 32 Issued 1, 2018.
- [53] S. Pölsterl, "scikit-survival: A Library for Time-to-Event Analysis Built on Top of scikit-learn," *Journal of Machine Learning Research*, vol. 21, no. 212, pp. 1–6, 2020. [Online]. Available: <http://jmlr.org/papers/v21/20-729.html>
- [54] P. Chapfuwa, C. Tao, C. Li, I. Khan, K. J. Chandross, M. J. Pencina, L. Carin, and R. Henao, "Calibration and Uncertainty in Neural Time-to-Event Modeling," *IEEE Transactions on Neural Networks and Learning Systems*, vol. 34, no. 4, pp. 1666–1680, 2023.
- [55] A. D. Palma, R. Bunel, K. Dvijotham, M. P. Kumar, and R. Stanforth, "IBP Regularization for Verified Adversarial Robustness via Branch-and-Bound," 2023.
- [56] A. Madry, A. Makelov, L. Schmidt, D. Tsipras, and A. Vladu, "Towards Deep Learning Models Resistant to Adversarial Attacks," 2019.
- [57] S. Goyal, K. Dvijotham, R. Stanforth, R. Bunel, C. Qin, J. Uesato, R. Arandjelovic, T. A. Mann, and P. Kohli, "On the Effectiveness of Interval Bound Propagation for Training Verifiably Robust Models," *CoRR*, vol. abs/1810.12715, 2018. [Online]. Available: <http://arxiv.org/abs/1810.12715>
- [58] K. Xu, Z. Shi, H. Zhang, Y. Wang, K.-W. Chang, M. Huang, B. Kailkhura, X. Lin, and C.-J. Hsieh, "Automatic Perturbation Analysis for Scalable Certified Robustness and Beyond," 2020.
- [59] I. J. Goodfellow, J. Shlens, and C. Szegedy, "Explaining and harnessing adversarial examples," *arXiv preprint arXiv:1412.6572*, 2014.
- [60] E. Rusak, L. Schott, R. S. Zimmermann, J. Bitterwolf, O. Bringmann, M. Bethge, and W. Brendel, "A simple way to make neural networks robust against diverse image corruptions," in *Computer Vision—ECCV 2020: 16th European Conference, Glasgow, UK, August 23–28, 2020, Proceedings, Part III 16*. Springer, 2020, pp. 53–69.
- [61] Zhang, Guojun, "Understanding Minimax Optimization in Modern Machine Learning," Ph.D. dissertation, University of Waterloo, 2021. [Online]. Available: <http://hdl.handle.net/10012/17157>
- [62] D. P. Kingma and J. Ba, "Adam: A method for stochastic optimization," 2017.
- [63] Y. Yao, L. Rosasco, and A. Caponnetto, "On Early Stopping in Gradient Descent Learning," *Constructive Approximation*, vol. 26, no. 2, pp. 289–315, August 1 2007. [Online]. Available: <https://doi.org/10.1007/s00365-006-0663-2>
- [64] J. Harrell, Frank E., R. M. Califf, D. B. Pryor, K. L. Lee, and R. A. Rosati, "Evaluating the Yield of Medical Tests," *JAMA*, vol. 247, no. 18, pp. 2543–2546, 05 1982. [Online]. Available: <https://doi.org/10.1001/jama.1982.03320430047030>
- [65] E. Graf, C. Schmoor, W. Sauerbrei, and M. Schumacher, "Assessment and comparison of prognostic classification schemes for survival data," *Statistics in Medicine*, vol. 18, no. 17-18, pp. 2529–2545, 1999.
- [66] C. Davidson-Pilon, "lifelines: survival analysis in python," *Journal of Open Source Software*, vol. 4, no. 40, p. 1317, 2019. [Online]. Available: <https://doi.org/10.21105/joss.01317>
- [67] E. Drysdale, "SurvSet: An open-source time-to-event dataset repository," 2022.
- [68] G. V. H. Jensen, C. Torp-Pedersen, P. Hildebrandt, L. Kober, F. Nielsen, T. Melchior, T. Joen, and P. Andersen, "Does in-hospital ventricular fibrillation affect prognosis after myocardial infarction?" *European heart journal*, vol. 18, no. 6, pp. 919–924, 1997.
- [69] "Stage C Prostate Cancer," <https://rdrr.io/cran/rpart/man/stagec.html>.
- [70] R. A. Kyle, T. M. Therneau, S. V. Rajkumar, D. R. Larson, M. F. Plevak, J. R. Offord, A. Dispenzieri, J. A. Katzmann, and L. J. Melton III, "Prevalence of monoclonal gammopathy of undetermined significance," *New England Journal of Medicine*, vol. 354, no. 13, pp. 1362–1369, 2006.
- [71] B. D. Ripley, *Modern applied statistics with S*. springer, 2002.
- [72] T. J. Wang, J. M. Massaro, D. Levy, R. S. Vasan, P. A. Wolf, R. B. D'Agostino, M. G. Larson, W. B. Kannel, and E. J. Benjamin, "A risk score for predicting stroke or death in individuals with new-onset atrial fibrillation in the community: the framingham heart study," *Jama*, vol. 290, no. 8, pp. 1049–1056, 2003.
- [73] "dataDIVAT1," <https://rdrr.io/cran/RISCA/man/dataDIVAT1.html>.
- [74] "Prostate dataset," <https://hbiostat.org/data/repo/cprostate>.
- [75] C. C. Abnet, B. Lai, Y.-L. Qiao, S. Vogt, X.-M. Luo, P. R. Taylor, Z.-W. Dong, S. D. Mark, and S. M. Dawsey, "Zinc concentration in esophageal biopsy specimens measured by x-ray fluorescence and esophageal cancer risk," *Journal of the National Cancer Institute*, vol. 97, no. 4, pp. 301–306, 2005.
- [76] A. Blair, D. Hadden, J. Weaver, D. Archer, P. Johnston, and C. Maguire, "The 5-year prognosis for vision in diabetes," *The Ulster medical journal*, vol. 49, no. 2, p. 139, 1980.
- [77] R. Henderson, S. Shimakura, and D. Gorst, "Modeling spatial variation in leukemia survival data," *Journal of the American Statistical Association*, vol. 97, no. 460, pp. 965–972, 2002.



Michael Potter is a Ph.D. student at Northeastern University under the advisement of Deniz Erdoğan of the Cognitive Systems Laboratory (CSL). He received his B.S., M.S., and M.S. degrees in Electrical and Computer Engineering from Northeastern University and University of California Los Angeles (UCLA) in 2020, 2020, and 2022 respectively. His research interests are in recommendation systems, Bayesian Neural Networks, uncertainty quantification, and dynamics based manifold learning.



Stefano Maxenti is a Ph.D. student in Computer Engineering at the Institute for the Wireless Internet of Things (WIoT) at Northeastern University, under the supervision of Prof. Tommaso Melodia. He received a B.Sc. in Engineering of Computing Systems in 2020 and a M.Sc. in Telecommunication Engineering in 2023 from Politecnico di Milano, Italy. He is interested in the application of AI to the field of networks and communications, specifically linked with O-RAN in 5G/6G.



Michael Everett received the S.B., S.M., and Ph.D. degrees in mechanical engineering from the Massachusetts Institute of Technology (MIT), Cambridge, MA, USA, in 2015, 2017, and 2020, respectively. He was a Post-Doctoral Associate and Research Scientist in the Department of Aeronautics and Astronautics at MIT. He was a Visiting Faculty Researcher at Google Research. He joined Northeastern University in 2023, where he is currently an Assistant Professor in the Department of Electrical & Computer Engineering and Khoury College of Computer Sciences at Northeastern University, Boston, MA, USA. His research lies at the intersection of machine learning, robotics, and control theory, with specific interests in the theory and application of safe and robust neural feedback loops. Dr. Everett's work has been recognized with numerous awards, including the Best Paper Award in Cognitive Robotics at IEEE/RSJ International Conference on Intelligent Robots and Systems (IROS) 2019.

APPENDIX

We find that as the ϵ -perturbation magnitude increases from 0 to 1, the relative percentage change from the baseline to the adversarial training methods becomes larger and then smaller. The relative percent changes from the baseline to SAWAR for ϵ equal to 1.0, 0.9, 0.8, 0.7, 0.6, 0.5, 0.4, 0.3, 0.2, 0.1, 0.05, 0 is 29.46, 48.18, 56.27, 72.23, 102.44, 133.35, 152.17, 140.33, 91.78, 21.17, 9.63, 1.07 respectively. We note that for very large ϵ , since our data is standard normalized all methods begin to fail.

	ϵ	1.00	0.90	0.80	0.70	0.60	0.50	0.40	0.30	0.20	0.10	0.05	0.00
Aids2	baseline	0.499	0.497	0.501	0.505	0.507	0.509	0.517	0.535	0.565	0.573	0.573	0.572
	noise	0.492	0.494	0.496	0.5	0.5	0.498	0.507	0.526	0.556	0.556	0.554	0.554
	fgsm	0.498	0.495	0.498	0.497	0.5	0.502	0.508	0.529	0.554	0.557	0.555	0.553
	pgd	0.498	0.497	0.497	0.5	0.501	0.501	0.507	0.531	0.557	0.558	0.556	0.554
	SAWAR	0.567	0.575	0.577	0.579	0.58	0.58	0.579	0.579	0.579	0.579	0.579	0.579
Framingham	baseline	0.612	0.623	0.635	0.646	0.656	0.664	0.672	0.678	0.682	0.686	0.687	0.688
	noise	0.606	0.616	0.626	0.635	0.642	0.649	0.659	0.674	0.683	0.685	0.685	0.685
	fgsm	0.607	0.611	0.617	0.622	0.626	0.635	0.652	0.669	0.682	0.686	0.687	0.686
	pgd	0.567	0.578	0.588	0.599	0.61	0.624	0.642	0.659	0.68	0.688	0.688	0.687
	SAWAR	0.694	0.697	0.699	0.701	0.702	0.704	0.704	0.705	0.705	0.704	0.704	0.704
LeukSurv	baseline	0.611	0.616	0.623	0.623	0.627	0.631	0.63	0.631	0.63	0.624	0.624	0.626
	noise	0.552	0.557	0.562	0.566	0.569	0.574	0.587	0.61	0.628	0.627	0.621	0.617
	fgsm	0.546	0.549	0.554	0.563	0.561	0.566	0.583	0.602	0.624	0.624	0.621	0.62
	pgd	0.537	0.536	0.538	0.549	0.546	0.558	0.577	0.598	0.62	0.622	0.619	0.617
	SAWAR	0.483	0.498	0.51	0.532	0.553	0.583	0.589	0.607	0.617	0.623	0.632	0.636
TRACE	baseline	0.564	0.586	0.612	0.637	0.665	0.69	0.714	0.73	0.734	0.733	0.735	0.735
	noise	0.565	0.588	0.613	0.64	0.668	0.692	0.716	0.73	0.733	0.735	0.734	0.735
	fgsm	0.553	0.577	0.603	0.63	0.658	0.688	0.713	0.722	0.727	0.73	0.733	0.734
	pgd	0.557	0.582	0.609	0.636	0.664	0.696	0.723	0.731	0.733	0.732	0.733	0.733
	SAWAR	0.73	0.733	0.736	0.738	0.739	0.739	0.74	0.74	0.739	0.738	0.738	0.737
dataDIVAT1	baseline	0.534	0.558	0.583	0.606	0.624	0.639	0.65	0.658	0.662	0.664	0.664	0.664
	noise	0.534	0.539	0.551	0.571	0.587	0.612	0.636	0.656	0.654	0.64	0.635	0.631
	fgsm	0.575	0.585	0.594	0.606	0.617	0.628	0.638	0.644	0.651	0.643	0.638	0.635
	pgd	0.517	0.529	0.548	0.568	0.591	0.618	0.636	0.654	0.657	0.651	0.647	0.644
	SAWAR	0.627	0.642	0.652	0.658	0.659	0.659	0.659	0.658	0.657	0.656	0.656	0.655
flchain	baseline	0.096	0.098	0.102	0.107	0.114	0.127	0.156	0.461	0.9	0.916	0.922	0.924
	noise	0.096	0.099	0.104	0.112	0.127	0.164	0.335	0.768	0.912	0.921	0.923	0.923
	fgsm	0.102	0.116	0.159	0.288	0.599	0.852	0.91	0.917	0.923	0.927	0.927	0.925
	pgd	0.102	0.127	0.235	0.538	0.824	0.904	0.917	0.921	0.925	0.929	0.929	0.929
	SAWAR	0.84	0.925	0.927	0.929	0.93	0.93	0.929	0.929	0.93	0.93	0.931	0.931
prostate	baseline	0.412	0.419	0.426	0.447	0.463	0.49	0.53	0.581	0.614	0.635	0.639	0.643
	noise	0.49	0.503	0.514	0.524	0.533	0.541	0.553	0.566	0.576	0.572	0.577	0.576
	fgsm	0.514	0.522	0.526	0.536	0.541	0.549	0.558	0.573	0.582	0.596	0.596	0.596
	pgd	0.522	0.526	0.532	0.535	0.54	0.548	0.557	0.567	0.576	0.593	0.591	0.593
	SAWAR	0.575	0.584	0.598	0.6	0.608	0.632	0.638	0.638	0.639	0.641	0.642	0.644
retinopathy	baseline	0.525	0.539	0.562	0.569	0.587	0.592	0.592	0.599	0.605	0.601	0.604	0.605
	noise	0.526	0.545	0.561	0.57	0.581	0.588	0.588	0.6	0.603	0.6	0.604	0.606
	fgsm	0.47	0.485	0.51	0.536	0.569	0.578	0.591	0.6	0.599	0.602	0.606	0.607
	pgd	0.471	0.481	0.509	0.53	0.567	0.577	0.591	0.599	0.598	0.601	0.606	0.607
	SAWAR	0.588	0.597	0.611	0.616	0.619	0.615	0.621	0.62	0.62	0.619	0.617	0.617
stagec	baseline	0.442	0.457	0.476	0.495	0.514	0.548	0.582	0.668	0.721	0.697	0.688	0.688
	noise	0.471	0.481	0.505	0.49	0.514	0.534	0.582	0.697	0.721	0.712	0.688	0.697
	fgsm	0.423	0.438	0.447	0.471	0.51	0.567	0.62	0.663	0.688	0.678	0.688	0.688
	pgd	0.462	0.486	0.471	0.495	0.51	0.567	0.611	0.668	0.692	0.688	0.697	0.697
	SAWAR	0.428	0.447	0.481	0.514	0.567	0.639	0.673	0.692	0.702	0.692	0.692	0.707
zinc	baseline	0.339	0.349	0.356	0.376	0.427	0.507	0.657	0.758	0.796	0.796	0.792	0.793
	noise	0.315	0.329	0.339	0.376	0.424	0.545	0.704	0.778	0.791	0.805	0.806	0.81
	fgsm	0.339	0.357	0.384	0.439	0.55	0.657	0.738	0.776	0.787	0.804	0.809	0.812
	pgd	0.333	0.351	0.384	0.439	0.55	0.671	0.738	0.776	0.79	0.8	0.809	0.808
	SAWAR	0.383	0.464	0.533	0.649	0.707	0.746	0.766	0.779	0.789	0.787	0.795	0.8

TABLE IV: Concordance Index metric for *SurvSet* datasets (higher is better) for each adversarial training method against the worst-case adversarial attack.

We find that as the ϵ -perturbation magnitude increases from 0 to 1, the relative percentage change from the baseline to the adversarial training methods becomes larger and then smaller. The relative percent changes from the baseline to SAWAR for ϵ equal to 1.0, 0.9, 0.8, 0.7, 0.6, 0.5, 0.4, 0.3, 0.2, 0.1, 0.05, 0 is -44.13, -45.46, -46.68, -47.57, -47.86, -47.10, -45.03, -40.89, -33.06, -20.29, -11.34, -1.68 respectively (where lower percentage change is better). We note that for very large ϵ , since our data is standard normalized all methods begin to fail.

	ϵ	1.00	0.90	0.80	0.70	0.60	0.50	0.40	0.30	0.20	0.10	0.05	0.00
Aids2	baseline	0.24	0.233	0.224	0.212	0.197	0.178	0.157	0.137	0.124	0.12	0.121	0.122
	noise	0.254	0.253	0.25	0.245	0.236	0.22	0.196	0.161	0.13	0.121	0.121	0.122
	fgsm	0.252	0.249	0.244	0.236	0.223	0.203	0.176	0.145	0.125	0.121	0.121	0.121
	pgd	0.252	0.248	0.243	0.234	0.221	0.2	0.172	0.143	0.124	0.121	0.121	0.121
	SAWAR	0.126	0.124	0.124	0.124	0.123	0.123	0.123	0.123	0.123	0.123	0.123	0.123
Framingham	baseline	0.81	0.8	0.778	0.733	0.65	0.52	0.369	0.243	0.165	0.128	0.119	0.115
	noise	0.818	0.818	0.816	0.809	0.778	0.681	0.495	0.294	0.174	0.128	0.119	0.116
	fgsm	0.818	0.816	0.81	0.791	0.728	0.58	0.369	0.208	0.14	0.12	0.116	0.115
	pgd	0.818	0.818	0.817	0.811	0.784	0.683	0.461	0.235	0.138	0.117	0.115	0.115
	SAWAR	0.165	0.152	0.141	0.133	0.127	0.122	0.118	0.116	0.114	0.114	0.113	0.113
LeukSurv	baseline	0.163	0.163	0.163	0.163	0.162	0.161	0.156	0.144	0.126	0.109	0.105	0.103
	noise	0.163	0.163	0.163	0.163	0.163	0.163	0.163	0.163	0.157	0.134	0.12	0.114
	fgsm	0.163	0.163	0.163	0.163	0.163	0.163	0.163	0.161	0.148	0.122	0.114	0.111
	pgd	0.163	0.163	0.163	0.163	0.163	0.163	0.163	0.16	0.145	0.12	0.114	0.111
	SAWAR	0.154	0.15	0.144	0.136	0.128	0.12	0.115	0.112	0.11	0.107	0.107	0.106
TRACE	baseline	0.634	0.634	0.633	0.626	0.603	0.549	0.449	0.329	0.234	0.183	0.172	0.167
	noise	0.634	0.634	0.632	0.622	0.596	0.536	0.435	0.319	0.23	0.183	0.172	0.167
	fgsm	0.634	0.634	0.634	0.631	0.613	0.555	0.434	0.294	0.212	0.177	0.171	0.168
	pgd	0.634	0.634	0.632	0.621	0.58	0.491	0.362	0.245	0.189	0.171	0.167	0.166
	SAWAR	0.282	0.254	0.231	0.213	0.198	0.186	0.177	0.17	0.166	0.163	0.163	0.163
dataDIVAT1	baseline	0.721	0.702	0.67	0.616	0.531	0.417	0.308	0.234	0.195	0.18	0.178	0.178
	noise	0.749	0.749	0.748	0.748	0.743	0.72	0.626	0.413	0.248	0.198	0.192	0.192
	fgsm	0.749	0.749	0.748	0.747	0.74	0.699	0.547	0.322	0.215	0.193	0.192	0.192
	pgd	0.749	0.749	0.749	0.748	0.746	0.724	0.582	0.305	0.192	0.184	0.186	0.187
	SAWAR	0.266	0.241	0.224	0.212	0.202	0.193	0.187	0.183	0.18	0.178	0.178	0.178
flchain	baseline	0.831	0.831	0.831	0.831	0.831	0.83	0.829	0.818	0.486	0.096	0.07	0.052
	noise	0.831	0.831	0.831	0.831	0.831	0.83	0.829	0.807	0.25	0.087	0.063	0.052
	fgsm	0.831	0.831	0.831	0.83	0.83	0.828	0.707	0.146	0.094	0.06	0.054	0.051
	pgd	0.831	0.831	0.831	0.83	0.83	0.797	0.298	0.114	0.079	0.055	0.051	0.05
	SAWAR	0.522	0.161	0.076	0.063	0.057	0.054	0.052	0.051	0.05	0.05	0.049	0.049
prostate	baseline	0.53	0.529	0.528	0.526	0.519	0.505	0.475	0.418	0.335	0.256	0.231	0.218
	noise	0.53	0.53	0.53	0.53	0.53	0.53	0.53	0.528	0.477	0.371	0.325	0.296
	fgsm	0.53	0.53	0.53	0.53	0.53	0.53	0.529	0.509	0.413	0.29	0.257	0.246
	pgd	0.53	0.53	0.53	0.53	0.53	0.53	0.528	0.502	0.396	0.28	0.254	0.244
	SAWAR	0.508	0.482	0.441	0.393	0.348	0.309	0.278	0.251	0.229	0.214	0.209	0.205
retinopathy	baseline	0.662	0.657	0.645	0.621	0.582	0.522	0.43	0.324	0.244	0.203	0.196	0.195
	noise	0.662	0.657	0.645	0.622	0.583	0.523	0.432	0.326	0.245	0.204	0.196	0.195
	fgsm	0.656	0.646	0.626	0.597	0.556	0.493	0.401	0.301	0.232	0.201	0.196	0.197
	pgd	0.656	0.645	0.625	0.596	0.554	0.49	0.397	0.299	0.231	0.201	0.197	0.198
	SAWAR	0.526	0.484	0.436	0.385	0.334	0.29	0.254	0.228	0.211	0.203	0.202	0.202
stagec	baseline	0.505	0.505	0.505	0.504	0.502	0.486	0.431	0.329	0.211	0.175	0.181	0.192
	noise	0.505	0.505	0.505	0.504	0.502	0.485	0.432	0.338	0.216	0.175	0.181	0.192
	fgsm	0.505	0.505	0.505	0.503	0.494	0.458	0.382	0.268	0.174	0.161	0.169	0.178
	pgd	0.505	0.505	0.505	0.503	0.493	0.454	0.377	0.261	0.169	0.159	0.167	0.176
	SAWAR	0.491	0.476	0.45	0.408	0.354	0.296	0.24	0.195	0.168	0.16	0.162	0.167
zinc	baseline	0.907	0.907	0.905	0.899	0.882	0.823	0.652	0.368	0.18	0.109	0.096	0.09
	noise	0.908	0.907	0.907	0.904	0.893	0.838	0.625	0.32	0.168	0.109	0.096	0.089
	fgsm	0.907	0.907	0.904	0.892	0.839	0.659	0.365	0.194	0.124	0.095	0.089	0.086
	pgd	0.907	0.907	0.903	0.89	0.832	0.64	0.348	0.187	0.122	0.094	0.088	0.087
	SAWAR	0.72	0.609	0.476	0.352	0.26	0.198	0.159	0.132	0.113	0.1	0.096	0.094

TABLE V: Integrated Brier Score metric for *SurvSet* datasets (lower is better) for each adversarial training method against the worst-case adversarial attack.

	ϵ	1.00	0.90	0.80	0.70	0.60	0.50	0.40	0.30	0.20	0.10	0.05	0.00
Aids2	baseline	1.14e+04	7.22e+03	4.60e+03	2.87e+03	1.80e+03	1.16e+03	7.95e+02	6.06e+02	5.32e+02	5.16e+02	5.17e+02	5.19e+02
	noise	3.84e+05	1.61e+05	6.68e+04	2.78e+04	1.14e+04	4.42e+03	1.83e+03	8.54e+02	5.64e+02	5.20e+02	5.19e+02	5.21e+02
	fgsm	6.77e+04	3.50e+04	1.78e+04	8.89e+03	4.35e+03	2.14e+03	1.10e+03	6.66e+02	5.35e+02	5.19e+02	5.19e+02	5.20e+02
	pgd	5.49e+04	2.86e+04	1.49e+04	7.58e+03	3.79e+03	1.92e+03	1.02e+03	6.42e+02	5.31e+02	5.19e+02	5.19e+02	5.19e+02
	SAWAR	5.29e+02	5.24e+02	5.22e+02	5.22e+02	5.21e+02	5.21e+02	5.21e+02	5.21e+02	5.21e+02	5.21e+02	5.22e+02	5.22e+02
Framingham	baseline	1.47e+05	7.07e+04	3.42e+04	1.68e+04	8.47e+03	4.57e+03	2.79e+03	2.01e+03	1.68e+03	1.54e+03	1.51e+03	1.50e+03
	noise	1.27e+07	3.17e+06	8.03e+05	2.06e+05	5.38e+04	1.48e+04	4.92e+03	2.39e+03	1.72e+03	1.54e+03	1.51e+03	1.50e+03
	fgsm	1.95e+06	5.96e+05	1.84e+05	5.70e+04	1.81e+04	6.33e+03	2.84e+03	1.85e+03	1.58e+03	1.51e+03	1.50e+03	1.49e+03
	pgd	2.01e+07	4.36e+06	9.57e+05	2.13e+05	4.88e+04	1.21e+04	3.85e+03	1.97e+03	1.57e+03	1.50e+03	1.49e+03	1.49e+03
	SAWAR	1.66e+03	1.62e+03	1.58e+03	1.56e+03	1.53e+03	1.52e+03	1.50e+03	1.50e+03	1.49e+03	1.49e+03	1.49e+03	1.49e+03
LeukSurv	baseline	1.79e+07	4.80e+06	1.29e+06	3.48e+05	9.29e+04	2.53e+04	6.59e+03	1.77e+03	5.76e+02	3.10e+02	2.74e+02	2.58e+02
	noise	5.46e+23	1.79e+21	7.98e+18	2.52e+16	8.53e+13	1.88e+11	5.25e+08	2.35e+06	3.37e+04	2.60e+03	1.21e+03	7.21e+02
	fgsm	8.34e+16	1.79e+15	3.10e+13	4.86e+11	8.13e+09	1.49e+08	2.72e+06	7.03e+04	3.45e+03	6.20e+02	4.31e+02	3.59e+02
	pgd	1.28e+15	3.89e+13	1.03e+12	2.67e+10	7.96e+08	2.30e+07	7.01e+05	2.80e+04	1.98e+03	4.65e+02	3.58e+02	3.17e+02
	SAWAR	2.07e+04	8.38e+03	3.50e+03	1.45e+03	6.62e+02	3.45e+02	2.91e+02	2.70e+02	2.60e+02	2.54e+02	2.52e+02	2.50e+02
TRACE	baseline	4.56e+09	4.41e+08	4.44e+07	4.61e+06	5.31e+05	6.71e+04	9.88e+03	2.20e+03	9.05e+02	6.03e+02	5.53e+02	5.32e+02
	noise	9.11e+08	1.07e+08	1.34e+07	1.74e+06	2.43e+05	3.71e+04	6.63e+03	1.78e+03	8.35e+02	5.93e+02	5.51e+02	5.32e+02
	fgsm	2.01e+11	9.10e+09	4.31e+08	2.24e+07	1.26e+06	8.26e+04	7.79e+03	1.61e+03	7.45e+02	5.74e+02	5.47e+02	5.35e+02
	pgd	4.53e+08	4.81e+07	5.35e+06	6.12e+05	7.63e+04	1.07e+04	2.09e+03	8.37e+02	5.94e+02	5.40e+02	5.31e+02	5.26e+02
	SAWAR	8.79e+02	7.60e+02	6.82e+02	6.29e+02	5.94e+02	5.69e+02	5.53e+02	5.41e+02	5.33e+02	5.28e+02	5.27e+02	5.27e+02
dataDIVAT1	baseline	1.43e+04	8.36e+03	4.95e+03	3.01e+03	1.91e+03	1.31e+03	9.99e+02	8.51e+02	7.84e+02	7.56e+02	7.51e+02	7.49e+02
	noise	5.69e+08	7.64e+07	1.05e+07	1.44e+06	2.07e+05	3.17e+04	5.75e+03	1.61e+03	9.08e+02	7.81e+02	7.67e+02	7.64e+02
	fgsm	2.48e+08	3.36e+07	4.65e+06	6.56e+05	9.64e+04	1.54e+04	3.12e+03	1.14e+03	8.16e+02	7.65e+02	7.61e+02	7.60e+02
	pgd	1.85e+11	8.02e+09	3.47e+08	1.75e+07	9.39e+05	6.14e+04	5.80e+03	1.27e+03	8.03e+02	7.57e+02	7.56e+02	7.57e+02
	SAWAR	9.18e+02	8.55e+02	8.21e+02	8.00e+02	7.86e+02	7.75e+02	7.66e+02	7.59e+02	7.55e+02	7.52e+02	7.51e+02	7.51e+02
flchain	baseline	3.35e+23	9.34e+20	2.56e+18	7.37e+15	2.23e+13	6.82e+10	2.29e+08	9.33e+05	1.67e+04	2.03e+03	1.25e+03	1.09e+03
	noise	2.18e+35	1.20e+31	7.58e+26	4.68e+22	3.48e+18	2.65e+14	2.21e+10	6.77e+06	4.45e+04	1.96e+03	1.22e+03	1.11e+03
	fgsm	1.61e+20	3.47e+17	7.79e+14	1.86e+12	5.49e+09	4.02e+07	6.37e+05	1.86e+04	2.15e+03	1.15e+03	1.09e+03	1.08e+03
	pgd	1.30e+16	7.91e+13	4.93e+11	3.47e+09	4.60e+07	1.33e+06	4.93e+04	4.99e+03	1.45e+03	1.10e+03	1.08e+03	1.07e+03
	SAWAR	6.31e+03	2.22e+03	1.43e+03	1.19e+03	1.12e+03	1.09e+03	1.08e+03	1.07e+03	1.07e+03	1.07e+03	1.07e+03	1.07e+03
prostate	baseline	9.74e+05	3.22e+05	1.06e+05	3.58e+04	1.21e+04	4.25e+03	1.64e+03	7.62e+02	4.66e+02	3.70e+02	3.51e+02	3.44e+02
	noise	7.00e+20	5.05e+18	3.75e+16	2.85e+14	2.28e+12	2.03e+10	2.59e+08	9.04e+06	4.85e+05	6.66e+04	2.94e+04	1.37e+04
	fgsm	3.16e+14	1.04e+13	3.40e+11	1.16e+10	4.07e+08	1.52e+07	6.47e+05	3.56e+04	3.75e+03	1.03e+03	7.20e+02	5.82e+02
	pgd	8.84e+12	4.29e+11	2.18e+10	1.14e+09	5.94e+07	3.27e+06	1.92e+05	1.44e+04	1.91e+03	6.40e+02	5.00e+02	4.39e+02
	SAWAR	9.65e+03	3.88e+03	1.66e+03	8.48e+02	5.43e+02	4.30e+02	3.83e+02	3.59e+02	3.45e+02	3.37e+02	3.35e+02	3.34e+02
retinopathy	baseline	1.11e+04	5.64e+03	2.88e+03	1.51e+03	8.08e+02	4.64e+02	2.98e+02	2.18e+02	1.84e+02	1.70e+02	1.68e+02	1.67e+02
	noise	1.11e+04	5.61e+03	2.88e+03	1.51e+03	8.13e+02	4.68e+02	2.99e+02	2.19e+02	1.84e+02	1.70e+02	1.68e+02	1.68e+02
	fgsm	7.43e+03	3.89e+03	2.07e+03	1.12e+03	6.33e+02	3.86e+02	2.63e+02	2.03e+02	1.78e+02	1.68e+02	1.67e+02	1.68e+02
	pgd	7.30e+03	3.83e+03	2.04e+03	1.11e+03	6.25e+02	3.81e+02	2.60e+02	2.02e+02	1.77e+02	1.68e+02	1.67e+02	1.68e+02
	SAWAR	4.02e+02	3.31e+02	2.79e+02	2.41e+02	2.14e+02	1.95e+02	1.82e+02	1.74e+02	1.69e+02	1.67e+02	1.67e+02	1.67e+02
stagec	baseline	1.16e+06	2.94e+05	7.50e+04	1.85e+04	4.81e+03	1.28e+03	3.57e+02	1.14e+02	5.35e+01	4.10e+01	3.98e+01	3.97e+01
	noise	2.07e+06	4.93e+05	1.14e+05	2.73e+04	6.49e+03	1.61e+03	4.19e+02	1.25e+02	5.50e+01	4.10e+01	3.96e+01	3.95e+01
	fgsm	1.80e+05	5.45e+04	1.67e+04	5.23e+03	1.64e+03	5.30e+02	1.77e+02	7.43e+01	4.54e+01	3.96e+01	3.91e+01	3.92e+01
	pgd	1.54e+05	4.77e+04	1.47e+04	4.63e+03	1.47e+03	4.84e+02	1.69e+02	7.23e+01	4.48e+01	3.93e+01	3.89e+01	3.90e+01
	SAWAR	1.03e+03	5.79e+02	3.30e+02	1.94e+02	1.21e+02	8.21e+01	6.10e+01	4.88e+01	4.22e+01	3.89e+01	3.83e+01	3.81e+01
zinc	baseline	2.62e+06	5.85e+05	1.33e+05	3.13e+04	7.43e+03	1.87e+03	5.36e+02	2.03e+02	1.11e+02	8.26e+01	7.71e+01	7.46e+01
	noise	2.93e+07	4.72e+06	7.76e+05	1.32e+05	2.34e+04	4.45e+03	9.48e+02	2.56e+02	1.14e+02	8.17e+01	7.69e+01	7.53e+01
	fgsm	2.50e+06	4.44e+05	9.49e+04	2.11e+04	4.89e+03	1.24e+03	3.66e+02	1.44e+02	9.01e+01	7.66e+01	7.53e+01	7.57e+01
	pgd	2.55e+06	4.38e+05	8.27e+04	1.87e+04	4.43e+03	1.13e+03	3.40e+02	1.39e+02	8.88e+01	7.66e+01	7.55e+01	7.60e+01
	SAWAR	1.31e+03	7.77e+02	4.72e+02	2.98e+02	1.98e+02	1.42e+02	1.10e+02	9.21e+01	8.28e+01	7.87e+01	7.80e+01	7.78e+01

TABLE VI: Negative Log Likelihood metric for *SurvSet* datasets (lower is better) for each adversarial training method against the worst-case adversarial attack.